Research Square

Preprints are preliminary reports that have not undergone peer review. They should not be considered conclusive, used to inform clinical practice, or referenced by the media as validated information.

# Hydrogen Sulfide Restores SPC-Mediated Cardioprotection in Diabetic Rats: Role of SIRT1/Nrf2 Signaling-Modulated Mitochondrial Dysfunction and Oxidative Stress

**Jing Zhang**
Nanchang University
**Manying Shi**
Nanchang University
**Yanjuan Jiang**
Nanchang University
**Xiaozhong Li**
Nanchang University
**Siyuan Li**
Nanchang University
**Jianyong Ma**
Nanchang University
**Wengen Zhu**
Nanchang University
**Xiao Liu**
Nanchang University
**Meilin Wei**
Nanchang University
**Wei Tu**
Nanchang University
**Yunfeng Shen**
Nanchang University
**Jianping Liu**
Nanchang University
**Xiaoyang Lai**
Nanchang University
**Peng Yu** ( yu8220182@163.com )
The Second Affiated Hospital Of Nanchang University https://orcid.org/0000-0002-9405-7686

**Original investigation**

**Keywords:** Hydrogen sulfide, SPC-mediated cardioprotection, Diabetic rats, SIRT1/Nrf2 signaling, Mitochondrial dysfunction, Oxidative stress

**Posted Date:** September 2nd, 2020

**DOI:** https://doi.org/10.21203/rs.3.rs-54843/v1

**License:** This work is licensed under a Creative Commons Attribution 4.0 International License.
Read Full License

# Abstract

**Background:** Diabetic hearts are vulnerable to myocardial ischemia/reperfusion injury (IRI), but are insensitive to SPC, activating peroxiredoxins that confer cardioprotection. Exogenous $H_2S$ protects against myocardial IRI by inhibiting mitochondrial permeability transition pore opening and oxidative stress. This study aimed to explore the underlying mechanisms of recovery of SPC-induced cardioprotection by $H_2S$-regulated oxidative stress in diabetic rat hearts.

**Methods:** Streptozotocin-induced type 1 diabetes mellitus (T1DM) rats preconditioned with GYY4137 and EX527 were subjected to cardiac IRI. Myocardial infarct size, cardiac enzyme levels, cardiac morphology and functioning were measured after IRI. Mitochondrial structure and functioning in the heart tissue was detected by the levels of ATP, as well as the activities of complex I-IV using TEM and ELISA. Oxidative stress was estimated by the levels of 4-HNE, MPO, MDA and SOD. The expressions of SIRT1, Nrf2, HO-1 and Nox-4 in cardiac tissues were measured by western blotting.

**Results:** SPC treatment demonstrated loss of cardioprotection in diabetic hearts. Pretreatment with GYY4137 significantly restored cardioprotection by SPC treatment through decreasing infarct area and release of enzymes, improving myocardial damage and functioning, maintaining mitochondrial structure and functioning. More importantly, $H_2S$ restores SPC protection as evidenced by suppressed oxidative stress, which showed association with reduced levels of 4-HNE, MPO and MDA and increased levels of SOD. The mechanism assay substantiated that GYY4137 attenuated hyperglycemia-induced reduction of SIRT1 expression and Nrf2 and HO-1 activation and restored SPC-mediated cardioprotection in diabetic rats. Additionally, the upregulated expression level of SIRT1 and enhanced Nrf2/HO-1/Nox-2 signaling in GYY4137+SPC group were significantly reversed by EX527 pretreatment.

**Conclusion:** These results suggest that exogenous $H_2S$ restores SPC-induced cardioprotection via inhibition of oxidative stress by activating SIRT1-dependent Nrf2/HO-1/Nox-2 signaling pathway in diabetic myocardial IRI.


# Background

Diabetes mellitus (DM) patients complicated with ischemic heart disease (IHD) leads to heart failure and even death throughout the world[1]. After almost 30 years of research, it has reached to an opinion that diabetic patients are more vulnerable to myocardial ischemia/reperfusion injury (IRI) and less responsive to many therapeutic strategies, such as ischemic conditioning, remote ischemic conditioning and drug-induced conditioning [2]. Till date, there is limited effectiveness available with regard to present therapies for restoring cardioprotection in diabetic IRI, including restricting oxidative stress, mitochondrial dysfunction and inflammation [3]. Therefore, it is necessary for us to investigate and find new and effective strategies or technologies for treating patients with diabetes and IHD.

Our previous studies have revealed that sevoflurane postconditioning (SPC) has a protective effect on normal myocardium [4], but its effectiveness is compromised under hyperglycemia [5]. This might be due

to the damage of GSK-3β phosphorylation and its upstream signaling pathways of PI3K/AKT and ERK1/2 in the presence of diabetes [6]. Increasing evidence has indicated that combining with cobalt chloride or inhibition of dynamin-related protein 1 assists in effectively restoring the protective effect of sevoflurane on diabetic myocardium [7]. The mechanism involved in improving oxidative stress and protecting mitochondrial function still requires clarification.

Hydrogen sulfide ($H_2S$) is a highly diffusible gas transmitter that plays an important physiological and pathological role in cardiovascular system [8]. $H_2S$ in the body is catalyzed by cystathionine β-synthase (CBS), cystathionine-γ lyase (CSE) and 3-mercaptothiotransferase (3-MPST) [9]. $H_2S$ reduces oxidative stress and improves myocardial IRI by down-regulating NF-κB and JAK2-STAT3 signaling pathways[10]. $H_2S$ also improves the protective effects associated with ischemic preconditioning or post-processing on IRI in diabetic and elderly rats through a variety of mechanisms [11, 12], and inhibits endoplasmic reticulum stress, mPTP opening [13], and increased autophagy[14]. A previous study has shown that the expression of SIRT1 is low in diabetic cardiomyopathy. Furthermore, few other studies have found that exogenous $H_2S$ improved oxidative stress through SIRT1 and improved diabetic myocardial IRI-induced apoptosis through endoplasmic reticulum stress [15]. Of note, $H_2S$ also improved mitochondrial function through SIRT3 to further improve IRI-induced lung damage in type 1 DM model [11]. In addition, sevoflurane induced autophagy by SIRT1 to improve cardiomyocyte damage [16]. However, very little is known on their relationship and relative roles in combination treatment of SPC and $H_2S$ cardioprotection in diabetic IRI, and their underlying molecular mechanism remain elusive.

Hence, in the present study, exogenous supplementation of $H_2S$ restoring the expression of SIRT1 in DCM further increases cardioprotective effects of SPC in diabetic IRI was hypothesized. Also the roles and specific mechanisms of SIRT1, antioxidant pathways, and their involvement in potential mechanism of mitochondrial dysfunction under high glucose conditions were investigated.

# Methods

### Animals and induction of diabetes

Pathogen-free male Sprague-Dawley rats were supplied from medical laboratory animal center of Nanchang University and used at 230–250 grams. All the animal tests were approved by the Institutional Animal Care and Use Committee of Nanchang University and conducted in adherence with the guidelines for the Principles of Laboratory Animal Care and Use of Laboratory Animals published by NIH (NIH Publication, 8th Edition, 2011).

Diabetic rats were utilized three days after their arrival, and then treated by the intraperitoneal injection of 65 mg/kg streptozotocin (STZ, Sigma, USA, diluted in 0.1 Mcitrate buffer). The operation above being the induction of diabetes [17]. When glucose was higher than 16.7 mmol/L 1 week as well as the appearance of relevant symptoms (polydipsia, polyuria),the rats could be classified as successful diabetic models and selected for experiment [18, 19]. Detailed data of the food consumption (g/kg/d), water intake

(mL/kg/d) and body weight (BW) were recorded for the start (baseline) and the beginning of the ischemia (week 4). And the heart weight (HW) was measured at the end of reperfusion.

### Experimental Protocols

The rats were randomized into 6 groups as follows: Sham group: Type 1 diabetes (T1DM) rats implemented thoracotomy without IR; I/R group: T1DM rats subjected to IR; SPC: T1DM rats subjected to IR and 2.5% sevoflurane post-treatment; H: T1DM rats subjected to IR and treated with $H_2S$ donor GYY4137 ; SPC + H: T1DM rats subjected to IR and 2.5% sevoflurane post-treatment and treated with $H_2S$ donor GYY4137;SPC + H + EX527:T1DM rats subjected to IR and 2.5% sevoflurane post-treatment and treated with $H_2S$ donor GYY4137 combined with EX527. Five days before the start of the operative model of heart IRI,the group of H and SPC + H were injected intraperitoneally with 133 μmol/kg $H_2S$ donor GYY4137; the group of SPC + H + EX527 was injected intraperitoneally with 133 μmol/kg $H_2S$ donor GYY4137 and simultaneous injection of 5 mg/kg EX527. The time period of ischemia and reperfusion was 30 minutes and 120 minutes, respectively. As regards sevoflurane post-treatment, 2.5% sevoflurane was inhaled steadily for 15 minutes before reperfusion. At the end of reperfusion, blood samples were collected from the inferior vena cava. Ventricular tissue was promptly frozen in liquid nitrogen and stored at -80℃ until assayed.

### In Vivo Rat heart IRI model

T1DM rats were anesthetized by the intraperitoneal injection of pentobarbital sodium (50 mg/kg) and fixed on the operating table. In order to maintain a real-time monitor on the standard limb lead ECG, we connected the needle electrode to the machine. Subsequently, mechanical ventilation was carried out by an animal ventilator (Alcott Biotech, China). The ventilation frequency was 45 to 60 times per minute, the tidal volume 2 ml/kg, and the inspiration and expiration ratio was 1: 1. Then, the chests were opened and the hearts were exposed straightway. Through a left thoracic incision and a 6/0 non-invasive suture with a slipknot around the anterior descending branch of the left coronary artery, myocardial ischemia was induced. Thirty minutes later, the left ventricle turned into redness and the ST segment dropped after releasing the slip knot which meant it was a successful reperfusion model. The sham-treated rats underwent left thoracotomy only.

### Measurement of Plasma $H_2S$

$H_2S$ concentrations in plasma were evaluated within the end of reperfusion, using the methylene blue and the Griess methods. In short, homogenized (1:5 w/v) the left ventricle in phosphate-buffered saline (100 mM, pH 7.4, 1:5 w/v) and centrifuged (10 min at 10,000 g at 4 °C) them. Then the supernatants were extracted for the measurement of $H_2S$ concentration. Details for measurement of $H_2S$ concentration have been previously described [20].

### Determination of Infarct Size

The hearts were immediately removed from the perfusion device once the reperfusion ended. Then they were cut slightly into 5–6 pieces of around 2 mm thick tissue at -80℃ for 5 min. Well frozen, the slices were incubated in 1% 2,3,5-triphenyltetrazolium chloride (TTC, Sigma, USA) solution and washed

thoroughly with a proper amount of PBS buffer in a warm bath. A completely lightless environment could lead to a better staining result. After that, leave them to set with 10% formaldehyde for at least 24 hours. Under the above condition, they turned into two distinct colors, off-white and brick red, which represented infarcted area and non-infarcted area respectively. Apart from the color, Image-ProPlus6.0 image analysis software could distinguish the infarct area and the non-infarct zone. As for the myocardial infarction volume, its percentage could be represented by the ratio of myocardial infarction area to risk area.

### Measurement of myocardial CK-MB, LDH and cTnI

The level of creatine kinase-MB (CK-MB) lactate dehydrogenase (LDH) and cardiac troponin I (cTnI) was measured to indicate and evaluate the extent of myocardial injury. After 2 h of rat heart reperfusion, the left ventricular tissue was selected for the measurement. Dissolved it in normal saline as tissue homogenate and took out 10% of it for the centrifugation at 4℃, 3000 r/min for 15 min. Then the supernatant was extracted and collected. Myocardial CK-MB, LDH and cTnI levels were detected spectrophotometrically (Lightway PQY-01, JP) using commercial kits in a blinded manner according to the manufacturer's instruction (Jiancheng Bioengineering Institute, Nanjing, China).

### Echocardiography

The mice were lightly anesthetized with new sodium pentobarbital (50 mg/kg intraperitoneally) and in vivo transthoracic echocardiography of the left ventricle (LV) using a 14-MHz linear array scan head. For the aim of higher-resolution M-mode imagine, VEVO 770 (Visual sonics) was interfaced. Ejection fraction (EF), fractional shortening (FS)%, stroke volume (SV), left ventricular internal dimension in systole (LVIDs), left ventricular internal dimension in diastole (LVIDd), left ventricular posterior wall in systole (LVPWs), left ventricular posterior wall in diastole (LVPWd), interventricular septum in systole (IVSs) and interventricular septum in diastole (IVSd) were calculated.

### Histopathological Examination

For histological analysis, the left ventricle was collected immediately after reperfusion and then fixed in 4% paraformaldehyde solution. After soaking for more than 24 h, they were dehydrated with ethanol and sectioned (4-6um thickness). Subsequently, pieces were stained with HE and Masson trichrome to obtain the extent of the myocardial damage. To draw a more precise conclusion, we analyzed multiple sections of every heart and then averaged these numbers to obtain a single fibrosis/LV and leukocyte infiltration measurement.

### Electron Microscopy

Ventricular tissues fixed with pH 7.3 cacodylate buffer which contained 2 mM calcium chloride overnight at 4 °C. Then, rinsed the tissues with 0.15 M cacodylate buffer 2 times for 15 min each. Next, the tissues were fixed in 1% buffered osmium tetroxide for 1 h. After all samples were washed 3 times by the ultrapure water, we dehydrated it in a graded Ethanol series (50, 70, 90, 100%) for 10 min twice. The tissues were cut into ultra-thin sections (55–65 nm) with the ultramicrotome and were taken into the uranium acetate saturated alcohol solution and lead citrate. Finally, scanned samples and collected images with an electron microscopy (HITACHI HT7700).

### Mitochondrial ATP and activity analysis

As previously described by Palmer [21], subsarcolemmal (SSM) and interfibrillar (IFM) mitochondria which were the subpopulation of cardiac mitochondria were isolated for the analysis. Both of them could be obtained by the following operation. First, tissue was mixed with Tris-Cl buffer and centrifuged in 4°C at 600 g for 10 min. As for IFM, the initial pellet was supposed a treatment with trypsin (5 mg/g tissue). Then extracted the supernatant and centrifuged again in 4°C at 6000 g for 10 min for the yielder of pellet. Finally, the pellet was blended with storage buffer and used Bradford reagent (Bio-Rad) to determine the protein concentration. The ATP content could be easily measured by the ATP lite (Perkin Elmer) as to the manufacturer's instructions. Through specific donor acceptors, the enzyme activities were measured by spectrophotometer. Complexes I and II activities were monitored by the Rotenone sensitive NADH-oxidoreductase and succinate decyl ubiquinone DCPIP reductase, respectively. Both complex III and IV could be evaluated by Ubiquinol cytochrome-c reductase as per the protocol described previously [22].

### Immunohistochemistry Staining

The myocardial tissue samples were fixed in 10% neutral buffered formalin and embedded in paraffin. Subsequently, 3% hydrogen peroxide was used for the blockage of endogenous peroxidase. On the basis of the manufacturer's instructions (Cell Signaling Technology, Boston, MA, USA), anti-4HNE antibodies were used as the primary antibodies for immunohistochemical staining. Then the sections were incubated with secondary antibody for 30 min at room temperature after washing with PBS. Finally, a 3,3'-diaminobenzidine (DAB) staining (Merck KGaA, Darmstadt, Germany) was chosen for the detection of positive area. Six fields were randomly selected for each section and photographed at × 200 magnification (Olympus BX-63, Tokyo, JAPAN). The images were analyzed using Image-ProPlus6.0 image analysis software.

### Detection of myocardial MPO, MDA and SOD

As previously described, they were measured with commercially available kits (Merck KGaA, Darmstadt, Germany) [23]. To be more specific, myeloperoxidase (MPO) activity was determined by lucigenin-enhanced chemiluminescence. As for the MDA level and SOD of myocardial homogenates, they were assessed by spectrophotometer.

### Isolation of Nuclear and Cytoplasmic Proteins and Western Blotting

After collecting myocardial tissue, the nuclear and cytoplasmic proteins was isolated by the Nuclear and Cytoplasmic Protein Extraction Kit (Sangon Biotech, Shanghai, China). Then took out 30 μg Cytoplasmic and Nuclear Proteins samples respectively and mixed with buffer. 10% standard polyacrylamide gels were used to perform the SDS-PAGE, then 30–60 μg Cytoplasmic Proteins and 30–45 μg Nuclear Proteins were loaded onto the gels. The proteins would be electrophoretically transferred to polyvinylidene fluoride membranes (PVDF) later. The PVDFs were blocked on Tris-buffered saline with Tween-20 (TBST) buffer which contained 5% skimmed milk and incubated overnight at 4 °C with primary antibodies. The PVDF which contained Cytoplasmic Proteins incubated with primary antibodies Silent information regulator factor 2-related enzyme 1 (SIRT1, Abcam, Cambridge, UK), nuclear factor E2-related factor 2 (Nrf2, Cell

Signaling Technology, Danvers, USA), heme oxygenase-1 (HO-1, Cell Signaling Technology, Danvers, USA), NADPH Oxidase-2 (Nox-2, Cell Signaling Technology, Danvers, USA) and glyceraldehyde-3 phosphate dehydrogenase (GAPDH, Beyotime Biotechnology, Shanghai, China). The PVDF which contained Nuclear Proteins incubated with primary antibodies SIRT1, Nrf2 and Histone H3 (Abcam, Cambridge, UK). After rinsing with TBST for three times, the membranes were incubated with goat anti-rabbit immunoglobulin G-horseradish peroxidase (1:1,000; cat. no. A0208) for 1.5 h at room temperature. Subsequently, after rinsing, developing, grayscale scanning, the gray values of the band were analyzed by using Image-ProPlus6.0 image analysis software.

### Statistical analysis

Data were expressed as means ± standard deviation (SD). Data from experiments were analyzed and Intergroup comparisons were performed by the analysis of variance (ANOVA) test followed by Tukey multiple comparisons test. A value of $P$ 0.05 was considered statistically significant difference.

## Results

### Exogenous $H_2S$ donor GYY4137 enabled SPC to attenuate myocardial IRI-induced cardiac infarction size and cardiac dysfunction in diabetic rats but was abolished by SIRT1 inhibition

The characteristics of rats acquired in the experimental animals are shown in Fig. 1b-e. Compared with age-matched control rats, the type 1 diabetic rats after 4 weeks of STZ-induced diabetes showed characteristic symptoms of diabetes including polyphagia, polydipsia and hyperglycemia, as evident by increased food consumption, water intake and blood glucose levels (Fig. 1b-d, $P < 0.05$). In addition to these results, the levels of $H_2S$ in plasma were shown in Fig. 1e. The levels of $H_2S$ in I/R group and SPC group were significantly more than those in the Sham group, and the myocardial levels of $H_2S$ in H group, SPC + H group and SPC + H + EX527 group were further enhanced when compared with I/R group and SPC group (Fig. 1e, $P < 0.05$).

As shown in Fig. 2, the marker enzymes associated with infarction size and myocardial injury were measured to confirm the cardioprotective effect of SPC on myocardial diabetic IRI. The results showed that the myocardial infarction area was significantly increased in other groups when compared to Sham group (Fig. 2a-b, $P < 0.05$). Compared with I/R group, myocardial infarction area in diabetic rats treated with SPC showed no significant changes (Fig. 2a-b, $P > 0.05$), while myocardial infarction area of diabetic rats treated with exogenous $H_2S$ donor GYY4137 showed significant reduction (Fig. 2a-b, $P < 0.05$). After administration of SPC and exogenous $H_2S$ donor GYY4137, myocardial infarction area of diabetic rats in SPC + H group was further decreased (Fig. 2a-b, $P < 0.05$). However, the hearts of diabetic rats were treated after SPC by combining GYY4137 and SIRT1 signal pathway inhibitor EX527 in SPC + H + EX527 group. The results revealed that the myocardial infarction area of diabetic rats was remarkably increased (Fig. 2a-b, $P < 0.05$). Meanwhile, the HW and BW of diabetic rats were estimated. The BW in all groups showed no significant differences (Fig. 2c, $P > 0.05$). The differences of HW and HW/BW in all groups showed a similar trend with that of myocardial infarction area. The HW and HW/BW showed significant

elevation in other groups when compared to Sham group (Fig. 2d-e, $P < 0.05$). The HW and HW/BW showed no significant differences between I/R group and SPC group (Fig. 2d-e, $P > 0.05$). Compared with SPC group, the HW and HW/BW were found to be significantly reduced in H group, and further reduced in SPC + H group (Fig. 2d-e, $P < 0.05$). But the heart weight and HW/BW in SPC + H + EX527 group were obviously elevated as compared to SPC + H group (Fig. 2d-e, $P < 0.05$).

Simultaneously, the myocardial CK-MB, LDH and cTnI levels of diabetic rats were also detected. As shown in Fig. 2f-h, the CK-MB, LDH and cTnI levels of diabetic rats in other groups were obviously higher than those in Sham group (Fig. 2f-h, $P < 0.05$). Compared with I/R group, the CK-MB, LDH and cTnI levels of diabetic rats in SPC group showed no significant reduction (Fig. 2f-h, $P > 0.05$), while CK-MB, LDH and cTnI levels were significantly decreased in H group, and further inhibited in SPC + H group (Fig. 2f-h, $P < 0.05$). Nonetheless, after treatment with SPC, GYY4137 and EX527, the CK-MB, LDH and cTnI levels in SPC + H + EX527 group were significantly elevated when compared with SPC + H group (Fig. 2f-h, $P < 0.05$).

To further confirm the effects of GYY4137 on myocardial diabetic IRI and whether SIRT1 was involved in the cardioprotective effects of SPC and $H_2S$, cardiac function of all groups was detected by echocardiography and the representative M-mode echocardiograms of all groups were presented in Fig. 3a. Left ventricular systolic function was reflected by EF%, FS%, SV, LVIDs and LVIDd, left ventricular diastolic function was reflected by LVPWs and LVPWd, and cardiac remodeling function was observed by IVSs and IVSd. As shown in Fig. 3b-j, the results showed that EF%, FS%, SV, LVPWs, LVPWd, IVSs, IVSd were significantly lowered, while LVIDs, LVIDd were significantly increased in other groups than in Sham group (Fig. 3b-j, $P < 0.05$). These cardiac function indexes showed no statistical differences between I/R group and SPC group (Fig. 3b-j, $P > 0.05$), while SPC treatment did not improve cardiac function of diabetic rats. Compared with SPC group, EF%, FS%, SV, LVPWs, LVPWd, IVSs, and IVSd were significantly increased in H group, and further elevated in SPC + H group, while LVIDs and LVIDd were significantly decreased in H group, and further declined in SPC + H group (Fig. 3b-j, $P < 0.05$). In contrast, EF%, FS%, SV, LVPWs, LVPWd, IVSs, and IVSd in SPC + H + EX527 group were obviously inhibited as compared with SPC + H group, and LVIDs and LVIDd in SPC + H + EX527 group showed significant improvement as compared with SPC + H group (Fig. 3b-j, $P < 0.05$).

### Effects of SPC on myocardial damage and fibrosis in GYY4137 Treated Diabetic Rats with or without EX527 Treatment

As shown in Fig. 4, the area of fibrosis fraction and leucocyte infiltration were measured by histological analysis. HE and Masson staining showed that the structure of myocardial tissue in Sham group remained clear, the cardiomyocytes were arranged neatly, and no fibrosis fraction and leucocyte infiltration were observed. In I/R group, the cardiomyocytes were arranged in disordered manner, and enlarged. A mass of fibrosis fraction and leucocyte infiltration were observed in I/R group when compared to Sham group (Fig. 4, $P < 0.05$). After SPC administration, the area of fibrosis fraction and leucocyte infiltration of diabetic rats in the myocardium o SPC group showed no significant reduction when

compared to I/R group (Fig. 4, $P > 0.05$), and also SPC did not improve myocardial histological changes in diabetic rats after I/R. Nonetheless, after treatment with exogenous $H_2S$ donor GYY4137, the myocardial tissue showed a clearer structure, lighter myocardial damage, and lower area of fibrosis fraction and leucocyte infiltration in H group when compared to I/R group (Fig. 4, $P < 0.05$). Also the area of fibrosis fraction and leucocyte infiltration in the myocardium of diabetic rats in SPC + H group were further reduced when compared to I/R group (Fig. 4, $P < 0.05$). However, the myocardial tissue structure in SPC + H + EX527 group was worsened after administration of SIRT1 signaling pathway inhibitor EX527, while the myocardial area of fibrosis fraction and leucocyte infiltration of diabetic rats in SPC + H + EX527 group was significantly increased when compared with SPC + H group (Fig. 4, $P < 0.05$).

### Effects of SPC on mitochondrial structure and function in GYY4137 Treated Diabetic Rats with or without EX527 Treatment

SIRT1 is an important gene in mitochondrial biogenesis and function in the cardiomyocytes of rodents [24]. To further indicate that exogenous $H_2S$ restores SPC-induced cardioprotection via maintaining normal mitochondrial structure and function, myocardial ultrastructural structure, myocardial ATP content and mitochondrial respiratory chain complex I-IV in all groups were detected. As shown in Fig. 5a, cardiomyocytes in Sham group appeared in well-arranged sarcomeres and intercalated disc manner, as well as normal mitochondria with no swelling and intact cristae density. Consistent with the previous studies, the ultrastructural damages were worsened in I/R group and SPC group. After ischemic reperfusion, cardiac muscle tissue showed absence and edematous separation of sarcomeres, vacuolation of mitochondria with a more pronounced derangement and mitochondrial membrane and cristae disruption. Compared with I/R group, SPC treatment did not decrease myocardial ultrastructural damages in SPC group, while exogenous $H_2S$ donor GYY4137 inhibited myocardial ultrastructural damages in H group and combined application of SPC and GYY4137 further reduced the ultrastructural damages in SPC + H group, showing relatively parallel arrangement of sarcomeres and normal structure of the mitochondria. However, after SIRT1 signal pathway inhibitor EX527 treatment, myocardial ultrastructural was found to be obviously deteriorated in SPC + H + EX527 group (Fig. 5a).

Moreover, myocardial ATP content and mitochondrial respiratory chain complex I-IV in all groups demonstrated similar trend. The myocardial ATP content and complex I-IV activities were shown to be significantly decreased in other groups when compared to those in Sham group (Fig. 5b-f, $P < 0.05$). Compared with I/R group, myocardial ATP content and complex I-IV activities of diabetic rats in SPC group showed no significant increase (Fig. 5b-f, $P > 0.05$), while myocardial ATP content and complex I-IV activities were markedly increased in H group, and further elevated in SPC + H group (Fig. 5b-f, $P < 0.05$). Nonetheless, after combining the utilization of SPC, GYY4137 and EX527, myocardial ATP content and complex I-IV activities in SPC + H + EX527 group were markedly decreased as compared to SPC + H group (Fig. 5b-f, $P < 0.05$).

### SIRT1 resisted IRI-induced oxidative stress participates in restoring the effect of H2S to SPC cardioprotection in diabetic rats

Abnormal mitochondrial structure and functioning along with oxidative damage were induced by overproduction of ROS in rodents with diabetic hearts [25]. Next, immunohistochemistry was employed in experimental groups to investigate the levels of MPO, MDA and SOD after IRI insult of SPC treatment with GYY4137 in diabetic rats, and whether these effects were affected by SIRT1 inhibitor EX527. As shown in Fig. 6a-b, the relative 4-HNE levels in diabetic rats in other groups were significantly higher than in Sham group (Fig. 6b, $P < 0.05$). Compared with I/R group, the relative 4-HNE levels in SPC group showed no significant changes (Fig. 6b, $P > 0.05$), while the relative 4-HNE levels were obviously reduced in H group, and further decreased in SPC + H group (Fig. 6b, $P < 0.05$). Nonetheless, after treatment with SPC, GYY4137 and EX527, the relative 4-HNE levels in SPC + H + EX527 group were significantly enhanced as compared to SPC + H group (Fig. 6b, $P < 0.05$).

In addition, the biochemical markers of oxidative stress in all groups were detected and showed in Fig. 6c-e. The levels of MPO and MDA were significantly higher and the levels of SOD were obviously lower in other groups when compared to Sham group (Fig. 6c-e, $P < 0.05$). The levels of MPO, MDA and SOD showed no significant differences between I/R group and SPC group (Fig. 6c-e, $P > 0.05$), but the levels of biochemical markers in oxidative stress showed no change after SPC treatment. Compared with I/R group, the levels of MPO and MDA were significantly inhibited and the levels of SOD were significantly enhanced in H group, and the levels of MPO and MDA were further inhibited and the levels of SOD were further enhanced in SPC + H group (Fig. 6c-e, $P < 0.05$). However, after SPC treatment, GYY4137 combined with SIRT1 signaling pathway inhibitor EX527 was used for treatment in SPC + H + EX527 group, and the levels of MPO and MDA were significantly enhanced and the levels of SOD were remarkably inhibited when compared to SPC + H group (Fig. 6c-e, $P < 0.05$).

### Exogenous $H_2S$ restored SPC-induced cardioprotection through SIRT1-regulated Nrf2/HO-1/Nox-2 signaling pathway activation in diabetic heart IRI

To further determine the effects of exogenous $H_2S$ restoration in SPC-induced cardioprotection in diabetic hearts, the protein expression levels of SIRT1-regulated Nrf2/HO-1/Nox-2 signaling pathway were measured by western blotting. As shown in Fig. 7a-e, the expression levels of cytoplasmic fraction SIRT1, Nrf2 and HO-1 were obviously down-regulated and the expression levels of cytoplasmic fraction Nox-2 were significantly up-regulated in I/R group and SPC group when compared to Sham group (Fig. 7a-e, $P < 0.05$). In addition, compared to I/R group, the expression levels of cytoplasmic fraction SIRT1, Nrf2, HO-1 and Nox-2 in SPC group showed no significant change (Fig. 7, $P > 0.05$), while the expression levels of cytoplasmic fraction SIRT1, Nrf2, and HO-1 were obviously up-regulated and the expression levels of cytoplasmic fraction Nox-2 was significantly down-regulated in H group (Fig. 7a-e, $P < 0.05$), and the expression levels of cytoplasmic fraction SIRT1, Nrf2, and HO-1 were further up-regulated and the expression level of cytoplasmic fraction Nox-2 was further down-regulated in SPC + H group (Fig. 7a-e, $P < 0.05$). In contrast, diabetic rat hearts underwent treatment with GYY4137 combined and SIRT1 signaling pathway inhibitor EX527 after SPC treatment in SPC + H + EX527 group, and the expression levels of cytoplasmic fraction SIRT1, Nrf2, and HO-1 were significantly down-regulated and the expression levels of cytoplasmic fraction Nox-2 were significantly up-regulated (Fig. 7a-e, $P < 0.05$).

Simultaneously, the expression levels of nuclear fraction SIRT1 and Nrf2 were measured by western blotting and the results showed a similar trend as that of cytoplasmic fraction. As shown in Fig. 7f-h, compared with Sham group, the expression levels of nuclear fractions SIRT1 and Nrf2 were shown to be significantly down-regulated in I/R and SPC groups (Fig. 7f-h, $P < 0.05$). In addition, compared to I/R group, the expression levels of nuclear fraction SIRT1 and Nrf2 in SPC group showed significant up-regulation (Fig. 7f-h, $P > 0.05$), while the expression levels of nuclear fractions SIRT1 and Nrf2 were obviously up-regulated in H group (Fig. 7f-h, $P < 0.05$), and the expression levels of nuclear fractions SIRT1 and Nrf2 were further up-regulated in SPC + H group (Fig. 7f-h, $P < 0.05$). In contrary, diabetic rat hearts were treated with GYY4137 and SIRT1 signaling pathway inhibitor EX527 after SPC treatment in SPC + H + EX527 group, and the expression levels of nuclear fractions SIRT1 and Nrf2 were remarkably down-regulated (Fig. 7f-h, $P < 0.05$). Our study results showed that the expression and distribution of SIRT1and Nrf2 demonstrated apparent changes after SPC, GYY4137 and EX527 administration. In SPC + H + EX527 group, Nrf2 was promoted entry into the nucleus, resulting in the downstream expression of antioxidant HO-1/Nox-2 pathway changes, and SPC mediated cardioprotection in diabetic rats were finally restored.

# Discussion

Regardless of whether it is newly diagnosed or diagnosed diabetes, it is associated with poorer long-term outcomes after myocardial infarction in high-risk patients [26]. This is because diabetes or hyperglycemia can lead to a variety of signaling pathway obstacles, ultimately causing tissue and cell damage. This in turn reduces the effect on tissues and cell protection strategies, or makes drugs ineffective [27]. When diabetes is in particularly combined with target organ IRI, a variety of classic protective strategies such as ischemic conditioning, remote ischemic conditioning and drug conditioning demonstrated no protective effects on the occurrence of IRI in heart, kidney, and brain [28–30]. Recently, it has been found that inhibition of PI3K/AKT and JAK/STAT3 signaling pathways in diabetic myocardium acts as an important mechanism, in which SPC improves DCM with IRI ineffectively [31, 32]. Our research study revealed that exogenous supplementation of $H_2S$ has effectively restored the expression of SIRT1 if IRI occurs in DCM, and further increases the protective effects of SPC on IRI in DCM [15]. Treatment with GYY4173 alleviates cardiac dysfunction and restores cardioprotection by SPC through SIRT1 function improvement in the regulation of Nrf2 and expression of downstream proteins [33]. In this study, the cardioprotective effects induced by $H_2S$ and $H_2S$ combined with SPC were observed. To our knowledge, this is the first study to explore the relative role of STAT1/Nrf2 signaling modulated mitochondrial dysfunction and oxidative stress in $H_2S$ restored SPC mediated cardioprotection in diabetic rats.

It is commonly known that SPC plays an important role in restricting myocardial infarction, decreasing myocardial harm as well as dysfunction, reducing ventricular arrhythmias, abatement of apoptosis of cardiomyocytes, and finally avoiding heart failure. Studies have shown that SPC treatment obviously improves functional recovery, and the infarct size after IRI is reduced by nearly 50% [34]. SPC treatment improves myocardial ischemia-reperfusion injury via PI3K/AKT and ERKI/2 signaling pathways[35, 36].

Our study research suggested that P13K phosphorylates the 3-position hydroxyl group on the inositol ring to generate phosphatidylinositol triphosphate, which subsequently acts as a second messenger and activates AKT after phosphorylation. Activated AKT activates endothelial nitric oxide synthase (eNOS), promotes NO synthesis via cardiomyocytes, and reduces the expression of tumor necrosis factor-α (TNF-α), interleukin-1 (IL-1), interleukin-6 (IL-6) and other inflammatory factors, resulting in cardiac protection [37, 38]. SPC treatment essentially protects myocardial infarction, and avoids IRI injury through various molecular mechanisms, i.e. the activation of PI3K/AKT signaling pathway decreases in ROS, increases ERK and HO-1 expression and regulates the activity of pro- and anti-apoptotic pathways [39–42]. Previous studies have also suggested that SPC treatment can directly improve left ventricular systolic dysfunction [41]. Due to blood flow obstruction in the myocardium, myocardial I/R induce increased intracellular ROS production, leading to an imbalance in energy metabolism and increasing intracellular calcium levels. The improvement of cardiac contractile function is closely related to mitochondrial functioning [40]. This actually indicates that SPC treatment alleviates oxidative stress and mitochondrial dysfunction caused by IRI. SPC treatment showed no protective effects on oxidative stress and mitochondrial damage during IRI in diabetic myocardium, further causing SPC to be ineffective on diabetic myocardial IRI [41]. The study results revealed that correction of hyperglycemic state through insulin treatment aggravates, rather than prevents the harmful effects of diabetes on ischemic injury, leading to ineffective protection by SPC [5]. Further research has found that the above-mentioned drugs or treatments are ineffective mainly due to oxidative stress and mitochondrial damage [42]. Some researchers have found that the combined use of metformin and p38 MAP Kinase (p38 MAPK) inhibitor improved the heart function when diabetic myocardium has IRI [44]. We further found that exogenous supplementation of $H_2S$ indeed restores the protection of SPC to diabetic myocardial IRI.

$H_2S$ is associated with a variety of physiological functions [9]. The mechanism of $H_2S$ in preventing myocardial IRI aims to reduce calcium overload, apoptosis, inflammation, and oxidative stress [13]. This involves a variety of signaling pathways such as upregulated PI3K-AKT-GSK-3β signaling pathway and adenosine 5’-monophosphate-activated protein kinase/mammalian target of rapamycin (AMPK/mTOR) signaling pathway, increased ERK1/2 phosphorylation, decreased p38 MAPK and c-Jun N-terminal kinase (JNK) phosphorylation in myocardial IRI [14, 45]. Previous study has indicated that ischemic conditioning demonstrated cardiac protection in young hearts but invalid in aged hearts [13]. Also interestingly, $H_2S$ restored IRI protection of old tissues or organs by drugs or ischemic treatment. It is common that both elderly myocardial damage and diabetic myocardial damage have similar mechanisms, such as oxidative stress and mitochondrial damage.

SIRT1 is a nicotinamide adenine dinucleotide-dependent deacetylase [46] that played an important role in mammalian health and disease, and is usually involved in the regulation of many physiological functions, including cell senescence, gene transcription, energy balance, and oxidative stress. SIRT1 induces deacetylation of targets such as peroxisome proliferator-activated receptor γ coactiva-tor-1 (PGC-1), Forkhead box O3 (FOXO3), p53 and NF-κB demonstrated significant impact on mitochondrial function, apoptosis and inflammation [43]. A previous study has confirmed that exogenous $H_2S$ supplementation

improved DM related myocardial IRI via SIRT1 alleviated oxidative stress and endoplasmic reticulum stress-mediated apoptosis [48]. Moreover, it also improved mitochondrial function through SIRT3 activation, further improving lung IRI damage in type 1 DM [12]. Our research further confirmed that $H_2S$ restores SIRT1 expression in DCM, and the expression of SIRT1 in diabetic myocardial IRI was further increased when treated with $H_2S$ and SPC combination. In addition, EX527 was used as a specific inhibitor of SIRT1, effectively inhibiting the induction effects of $H_2S$ combined with SPC on SIRT1. Inhibition of SIRT1 not only restrains the protective effects of $H_2S$ on diabetic myocardial IRI, but also abrogates the protective effects of $H_2S$ combined with SPC. This is inseparable from the activation of downstream Nrf2 antioxidant pathway by SIRT1.

Nrf2 is a member of NF-E2 family of nuclear basic leucine zipper transcription factors [45]. $H_2S$ improves cardiac functioning of myocardial IRI and DCM by promoting the expression of Nrf2 [48, 50]. Nrf2 is activated and entered into the nucleus to further promote the expression of antioxidant factors or proteins, increasing the protein expression of HO-1 and HO-1 Trx1. Coptisine significantly promoted the expression of Nrf2 and increased its activity in improving $H_2O_2$-induced mitochondrial damage [51]. Moreover, some researchers have also found that Tricetin usage can activate Nrf2/HO-1 signaling pathway, which in turn protects mitochondrial function [52]. As a matter of fact, early studies have confirmed that both $H_2S$ and sevoflurane promoted the activation of Nrf2, and then exerted mitochondrial protection [42, 49]. Consistent with earlier research, we found that when SPC was used in combination with $H_2S$, the expression level of Nrf2 in the cytoplasm and nucleus was significantly increased, inducing the increased expression of antioxidant HO-1, and inhibiting the expression of pro-oxidant factor NOX-2. This assists SPC treatment to exert cardioprotective effect on IRI under hyperglycemic condition. We also observed that the combination treatment significantly inhibited the area of myocardial infarction in diabetic rats, reduced myocardial enzyme release, improved myocardial tissue damage, and effectively prevented the declination of cardiac functioning. Through TEM, we also observed that the ultrastructural damage of cardiomyocytes in diabetic rats was significantly improved and the integrity of myofilament and mitochondrial structure were protected after treatment with SPC combined with $H_2S$ during IRI in the heart of diabetic rats. Further analysis in our study confirmed that the ATP content and mitochondrial-related complex activity in the heart of diabetic rats in SPC combined with $H_2S$ treatment group were significantly increased when compared to IRI or SPC simple treatment group.

# Limitations

This study has few limitations that requires acknowledgement. Firstly, only preliminary experiments on animals were conducted using specific inhibitors to investigate mechanism experiments. Transgenic or knockout mice animal models or *in vitro* cell experiments to knock out or overexpress SIRT1 or Nrf2 to further assess the underlying mechanism should be adopted. Secondly, the present study is related to the experimental animal model of STZ-induced Type 1 diabetic rats. Although this model is widely accepted for screening anti-diabetic drugs, it does not fully represent the underlying mechanism of human type 2 DM. It is necessary to further clarify in a detailed manner whether the model can truly represent the

clinical manifestations of diabetic patients. Further use of high-fat-induced type 2 diabetes rats or db/db, ob/ob and other transgenic type 2 diabetes rats should be used for conducting research.

# Conclusion

In summary, the current results confirmed that SPC has no protective effects on diabetic myocardial IR. The study findings further indicated that advance $H_2S$ donor GYY4137 has effectively restored the diabetic myocardial protection of SPC within 5 days. Compared with pure $H_2S$ treatment, SPC combined with $H_2S$ has a stronger protective effect. As shown in Fig. 8, our results also illustrated that hyperglycemic-induced oxidative stress and mitochondria dysfunction led to SPC cardioprotection in diabetes by impairing SIRT1-modulated Nrf2/HO-1/Nox-2 signaling. What's more, the current study findings have provided further support to the hypothesis that $H_2S$ treatment and/or improvement of SIRT1-modulated Nrf2/HO-1 signaling pathway might act as useful approaches in attenuating diabetic myocardial IRI and preserving the effectiveness of therapeutic strategies, such as sevoflurane preconditioning or postconditioning.

# Abbreviations

DM: diabetes mellitus; IRI: ischaemia/reperfusion injury; CBS: cystathionine β-synthase; CSE: cystathionine-γ lyase; GSK-3b:Glycogen Synthase Kinase 3B; ERK1/2:extracellular regulated protein kinases1/2; NF-κB: nuclear factor kappa-B; JAK2-STAT3:Janus kinase2- signal transducer and activator of transcription 3; mPTP:1-Methyl-4-phenyl-1,2,3,6-tetrahydropyridin; SIRT1: silent information regulator-1; Nrf2:nuclear factor E2-related factor; DCM: diabetic cardiomyopathy; SPC: sevoflurane postconditioning; eNOS: endothelial nitric oxide synthase ROS: reactive oxygen species; ERK: extracellular signal-regulated kinase; HO-1:heme oxygenase-1; PI3K:phosphoinositide 3-kinases ; AKT: protein kinase b; H2S:Hydrogen sulfide; 3-MPST:3-mercaptothiotransferase; p38 MAPK:p38 MAP Kinase; JNK: c-Jun N-terminal kinase; AMPK: Adenosine 5’-Monophosphate-activated protein linase; mTOR: mammalian target of rapamycin;SIRT1:silent information regulato-1r; Nrf2:nuclear factor E2-related factor; Trx1:thioredxoin-1; Nox-4: NADPH Oxidase-4; NOX-2:NADPH Oxidase-2; H2S:Hydrogen sulfide; T1DM:Type 1 diabetes; CK-MB: cardiac kinase-MB; LDH: dehydrogenase; cTnI: cardiac troponin I; LV: left ventricle; EF: Ejection fraction; SV: stroke volume; LVIDs: left ventricular internal dimension in systole; LVIDd: left ventricular internal dimension in diastole; LVPWs: left ventricular posterior wall in systole; LVPWd: left ventricular posterior wall in diastole; IVSs: interventricular septum in systole; IVSd: interventricular septum in diastole; TNF-α: tumor necrosis factor-α; IL-1: Interleukin-1; IL-6: Interleukin-6; PGC − 1: peroxisome proliferator-activated receptor γ coactiva-tor-1; FOXO3: forkhead box O3; SSM: subsarcolemmal; IFM: interfibrillar; DAB:3,3'-diaminobenzidine; MPO: myeloperoxidase; MDA: malonaldehyde; SOD: superoxide dismutase; PVDF: polyvinylidene fluoride membranes; TBST: Tris buffered saline with Tween-20; STZ: streptozotocin; ATP: adenosine triphosphate; TEM: transmission electron microscope; 4-HNE: 4 –hydroxynonenal.

# Declarations

## Acknowledgements

Not applicable.

## Authors' contributions

JZ, MYS, QZ, SYL, JYM, WGZ and XL performed nearly all the experiments. MW and WT performed Hemodynamic study and analyzed the data. YFS, JPL, XYL and PY designed the whole study. PY, XZL and ZJ were the major contributors in writing the manuscript, and all the experiments were performed under their guidance. All authors read and approved the final manuscript.

## Funding

This study was supported by grants from the Natural Science Foundation in Jiangxi Province grant (20192ACBL21037 to P.Y.), the National Natural Science Foundation of China (81760048 to J.Z. and 81760050 to P.Y.)

## Availability of data and materials

The datasets used and/or analyzed during the current study are available from the corresponding author on reasonable request.

## Ethics approval and consent to participate

The animal protocols complied with the Guide of Care and the Use of Laboratory Animals published by the U.S. National Institutes of Health (NIH Publication, 8th Edition, 2011) and authorization was given by the Committee for Experimental Animals of Nanchang University.

## Consent for publication

Not applicable.

## Competing interests

The authors declare that they have no competing interests.

## Author details

1 Department of Anesthesiology, The Second Affiliated Hospital of Nanchang University□Jiangxi, Nanchang 330006, China□2 Department of Metabolism and Endocrinology, The Second Affiliated Hospital of Nanchang University□Jiangxi, Nanchang 330006, China□3 Department of Cardiology, The Second Affiliated Hospital of Nanchang University□Jiangxi, Nanchang, 330006, China□4 Grade 2017, The Second Clinical Medical College of Nanchang University, Nanchang, 330006, China□5 Department of Pharmacology and Systems Physiology, University of Cincinnati College of Medicine, Cincinnati, OH

45267, USA, 6 Department of Cardiology, the First Affiliated Hospital of Sun Yat-Sen University, Guangzhou, Guangdong, 510080, China.

# References

1. Rawshani A, Rawshani A, Franzen S, et al. Mortality and Cardiovascular Disease in Type 1 and Type 2 Diabetes. N Engl J Med. 2017;376(15):1407-1418.
2. Ansari M, Kurian GA. Hydrogen sulfide preconditioning could ameliorate reperfusion associated injury in diabetic cardiomyopathy rat heart through preservation of mitochondria. Biochimie. 2019;158:208-216.
3. Jia G, DeMarco VG, Sowers JR. Insulin resistance and hyperinsulinaemia in diabetic cardiomyopathy. Nat Rev Endocrinol. 2016;12(3):144-153.
4. Qiao S, Xie H, Wang C, Wu X, Liu H, Liu C. Delayed anesthetic preconditioning protects against myocardial infarction via activation of nuclear factor-kappaB and upregulation of autophagy. J Anesth. 2013;27(2):251-260.
5. Drenger B, Ostrovsky IA, Barak M, Nechemia-Arbely Y, Ziv E, Axelrod JH. Diabetes blockade of sevoflurane postconditioning is not restored by insulin in the rat heart: phosphorylated signal transducer and activator of transcription 3- and phosphatidylinositol 3-kinase-mediated inhibition. Anesthesiology. 2011;114(6):1364-1372.
6. Tai W, Shi E, Yan L, Jiang X, Ma H, Ai C. Diabetes abolishes the cardioprotection induced by sevoflurane postconditioning in the rat heart in vivo: roles of glycogen synthase kinase-3beta and its upstream pathways. J Surg Res. 2012;178(1):96-104.
7. Yu J, Maimaitili Y, Xie P, et al. High glucose concentration abrogates sevoflurane post-conditioning cardioprotection by advancing mitochondrial fission but dynamin-related protein 1 inhibitor restores these effects. Acta Physiol (Oxf). 2017;220(1):83-98.
8. Zhao K, Li H, Li S, Yang G. Regulation of cystathionine gamma-lyase/H(2)S system and its pathological implication. Front Biosci (Landmark Ed). 2014;19:1355-1369.
9. Li H, Mani S, Cao W, et al. Interaction of hydrogen sulfide and estrogen on the proliferation of vascular smooth muscle cells. PLoS One. 2012;7(8):e41614.
10. Li L, Li M, Li Y, et al. Exogenous H2S contributes to recovery of ischemic post-conditioning-induced cardioprotection by decrease of ROS level via down-regulation of NF-kappaB and JAK2-STAT3 pathways in the aging cardiomyocytes. Cell Biosci. 2016;6:26.
11. Zhang Y, Gao J, Sun W, et al. H2S restores the cardioprotective effects of ischemic post-conditioning by upregulating HB-EGF/EGFR signaling. Aging (Albany NY). 2019;11(6):1745-1758.
12. Jiang T, Liu Y, Meng Q, et al. Hydrogen sulfide attenuates lung ischemia-reperfusion injury through SIRT3-dependent regulation of mitochondrial function in type 1 diabetic rats. Surgery. 2019;165(5):1014-1026.

13. Li H, Zhang C, Sun W, et al. Exogenous hydrogen sulfide restores cardioprotection of ischemic post-conditioning via inhibition of mPTP opening in the aging cardiomyocytes. Cell Biosci. 2015;5:43.
14. Chen J, Gao J, Sun W, et al. Involvement of exogenous H2S in recovery of cardioprotection from ischemic post-conditioning via increase of autophagy in the aged hearts. Int J Cardiol. 2016;220:681-692.
15. Yu L, Li S, Tang X, et al. Diallyl trisulfide ameliorates myocardial ischemia-reperfusion injury by reducing oxidative stress and endoplasmic reticulum stress-mediated apoptosis in type 1 diabetic rats: role of SIRT1 activation. Apoptosis. 2017;22(7):942-954.
16. Fan L, Chen D, Wang J, Wu Y, Li D, Yu X. Sevoflurane Ameliorates Myocardial Cell Injury by Inducing Autophagy via the Deacetylation of LC3 by SIRT1. Anal Cell Pathol (Amst). 2017;2017:6281285.
17. Yin T, Hou R, Liu S, Lau WB, Wang H, Tao L. Nitrative inactivation of thioredoxin-1 increases vulnerability of diabetic hearts to ischemia/reperfusion injury. J Mol Cell Cardiol. 2010;49(3):354-361.
18. Yu LM, Di WC, Dong X, et al. Melatonin protects diabetic heart against ischemia-reperfusion injury, role of membrane receptor-dependent cGMP-PKG activation. Biochim Biophys Acta Mol Basis Dis. 2018;1864(2):563-578.
19. Shi Z, Fu F, Yu L, et al. Vasonatrin peptide attenuates myocardial ischemia-reperfusion injury in diabetic rats and underlying mechanisms. Am J Physiol Heart Circ Physiol. 2015;308(4):H281-290.
20. Shen X, Pattillo CB, Pardue S, Bir SC, Wang R, Kevil CG. Measurement of plasma hydrogen sulfide in vivo and in vitro. Free Radic Biol Med. 2011;50(9):1021-1031.
21. Palmer JW, Tandler B, Hoppel CL. Biochemical properties of subsarcolemmal and interfibrillar mitochondria isolated from rat cardiac muscle. J Biol Chem. 1977;252(23):8731-8739.
22. Ansari M , Kurian G A . Hydrogen sulfide preconditioning could ameliorate reperfusion associated injury in diabetic cardiomyopathy rat heart through preservation of mitochondria[J]. Biochimie, 2019, 158:208-216.
23. Erşahin M, Sehirli O, Toklu HZ, et al. Share Melatonin improves cardiovascular function and ameliorates renal, cardiac and cerebral damage in rats with renovascular hypertension. J Pineal Res. 2009;47(1):97-106.
24. Price NL, Gomes AP, Ling AJ, et al. SIRT1 is required for AMPK activation and the beneficial effects of resveratrol on mitochondrial function. Cell Metab. 2012;15(5):675-690.
25. Silzer T, Barber R, Sun J, et al. Circulating mitochondrial DNA: New indices of type 2 diabetes-related cognitive impairment in Mexican Americans. PLoS One. 2019;14(3):e0213527.
26. Aguilar D, Solomon SD, Kober L, et al. Newly diagnosed and previously known diabetes mellitus and 1-year outcomes of acute myocardial infarction: the VALsartan In Acute myocardial iNfarcTion (VALIANT) trial. Circulation. 2004;110(12):1572-1578.
27. Lejay A, Fang F, John R, et al. Ischemia reperfusion injury, ischemic conditioning and diabetes mellitus. J Mol Cell Cardiol. 2016;91:11-22.

28. Yu SY, Dong B, Fang ZF, Hu XQ, Tang L, Zhou SH. Knockdown of lncRNA AK139328 alleviates myocardial ischaemia/reperfusion injury in diabetic mice via modulating miR-204-3p and inhibiting autophagy. J Cell Mol Med. 2018;22(10):4886-4898.
29. Gong DJ, Wang L, Yang YY, Zhang JJ, Liu XH. Diabetes aggravates renal ischemia and reperfusion injury in rats by exacerbating oxidative stress, inflammation, and apoptosis. Ren Fail. 2019;41(1):750-761.
30. Lin M, Ling J, Geng X, Zhang J, Du J, Chen L. RTN1-C is involved in high glucose-aggravated neuronal cell subjected to oxygen-glucose deprivation and reoxygenation injury via endoplasmic reticulum stress. Brain Res Bull. 2019;149:129-136.
31. Wang T, Mao X, Li H, et al. N-Acetylcysteine and allopurinol up-regulated the Jak/STAT3 and PI3K/Akt pathways via adiponectin and attenuated myocardial postischemic injury in diabetes. Free Radic Biol Med. 2013;63:291-303.
32. Zhu Y, Pereira RO, O'Neill BT, et al. Cardiac PI3K-Akt impairs insulin-stimulated glucose uptake independent of mTORC1 and GLUT4 translocation. Mol Endocrinol. 2013;27(1):172-184.
33. Zheng Q, Pan L, Ji Y. H 2S protects against diabetes-accelerated atherosclerosis by preventing the activation of NLRP3 inflammasome. J Biomed Res. 2019;34(2):94-102.
34. Rahman S, Li J, Bopassa JC, et al. Phosphorylation of GSK-3beta mediates intralipid-induced cardioprotection against ischemia/reperfusion injury. Anesthesiology. 2011;115(2):242-253.
35. Xie H, Zhang J, Zhu J, et al. Sevoflurane post-conditioning protects isolated rat hearts against ischemia-reperfusion injury via activation of the ERK1/2 pathway. Acta Pharmacol Sin. 2014;35(12):1504-1513.
36. Zhang J, Wang C, Yu S, et al. Sevoflurane postconditioning protects rat hearts against ischemia-reperfusion injury via the activation of PI3K/AKT/mTOR signaling. Sci Rep. 2014;4:7317.
37. Alyahya AM, Al-Masri A, Hersi A, et al. The Effects of Progranulin in a Rat Model of Acute Myocardial Ischemia/Reperfusion are Mediated by Activation of the P13K/Akt Signaling Pathway. Med Sci Monit Basic Res. 2019;25:229-237.
38. Zhang X, Huang LF, Hua L, Feng HK, Shen B. Resveratrol protects myocardial apoptosis induced by ischemia-reperfusion in rats with acute myocardial infarction via blocking P13K/Akt/e-NOS pathway. Eur Rev Med Pharmacol Sci. 2019;23(4):1789-1796.
39. Ye Z, Guo Q, Xia P, Wang N, Wang E, Yuan Y. Sevoflurane postconditioning involves an up-regulation of HIF-1alpha and HO-1 expression via PI3K/Akt pathway in a rat model of focal cerebral ischemia. Brain Res. 2012;1463:63-74.
40. Yao YT, Li LH, Chen L, Wang WP, Li LB, Gao CQ. Sevoflurane postconditioning protects isolated rat hearts against ischemia-reperfusion injury: the role of radical oxygen species, extracellular signal-related kinases 1/2 and mitochondrial permeability transition pore. Mol Biol Rep. 2010;37(5):2439-2446.
41. Li H, Wang JK, Zeng YM, et al. Sevoflurane post-conditioning protects against myocardial reperfusion injury by activation of phosphatidylinositol-3-kinase signal transduction. Clin Exp Pharmacol Physiol.

2008;35(9):1043-1051.

42. Yu LN, Yu J, Zhang FJ, et al. Sevoflurane postconditioning reduces myocardial reperfusion injury in rat isolated hearts via activation of PI3K/Akt signaling and modulation of Bcl-2 family proteins. J Zhejiang Univ Sci B. 2010;11(9):661-672.
43. Doenst T, Nguyen TD, Abel ED. Cardiac metabolism in heart failure: implications beyond ATP production. Circ Res. 2013;113(6):709-724.
44. Jeremic JN, Jakovljevic VL, Zivkovic VI, et al. The cardioprotective effects of diallyl trisulfide on diabetic rats with ex vivo induced ischemia/reperfusion injury. Mol Cell Biochem. 2019;460(1-2):151-164.
45. Li H, Wang Y, Wei C, et al. Mediation of exogenous hydrogen sulfide in recovery of ischemic post-conditioning-induced cardioprotection via down-regulating oxidative stress and up-regulating PI3K/Akt/GSK-3beta pathway in isolated aging rat hearts. Cell Biosci. 2015;5:11.
46. Sinclair DA, Guarente L. Extrachromosomal rDNA circles--a cause of aging in yeast. Cell. 1997;91(7):1033-1042.
47. Poulose N, Raju R. Sirtuin regulation in aging and injury. Biochim Biophys Acta. 2015;1852(11):2442-2455.
48. Hu MZ, Zhou B, Mao HY, et al. Exogenous Hydrogen Sul fi de Postconditioning Protects Isolated Rat Hearts From Ischemia/Reperfusion Injury Through Sirt1/PGC-1alpha Signaling Pathway. Int Heart J. 2016;57(4):477-482.
49. Calvert JW, Jha S, Gundewar S, et al. Hydrogen sulfide mediates cardioprotection through Nrf2 signaling. Circ Res. 2009;105(4):365-374.
50. Hu X, Rajesh M, Zhang J, et al. Protection by dimethyl fumarate against diabetic cardiomyopathy in type 1 diabetic mice likely via activation of nuclear factor erythroid-2 related factor 2. Toxicol Lett. 2018;287:131-141.
51. Choi YH. Activation of the Nrf2/HO-1 signaling pathway contributes to the protective effects of coptisine against oxidative stress-induced DNA damage and apoptosis in HaCaT keratinocytes. Gen Physiol Biophys. 2019;38(4):281-294.
52. Ren J, Yuan L, Wang W, et al. Tricetin protects against 6-OHDA-induced neurotoxicity in Parkinson's disease model by activating Nrf2/HO-1 signaling pathway and preventing mitochondria-dependent apoptosis pathway. Toxicol Appl Pharmacol. 2019;378:114617.

# Figures

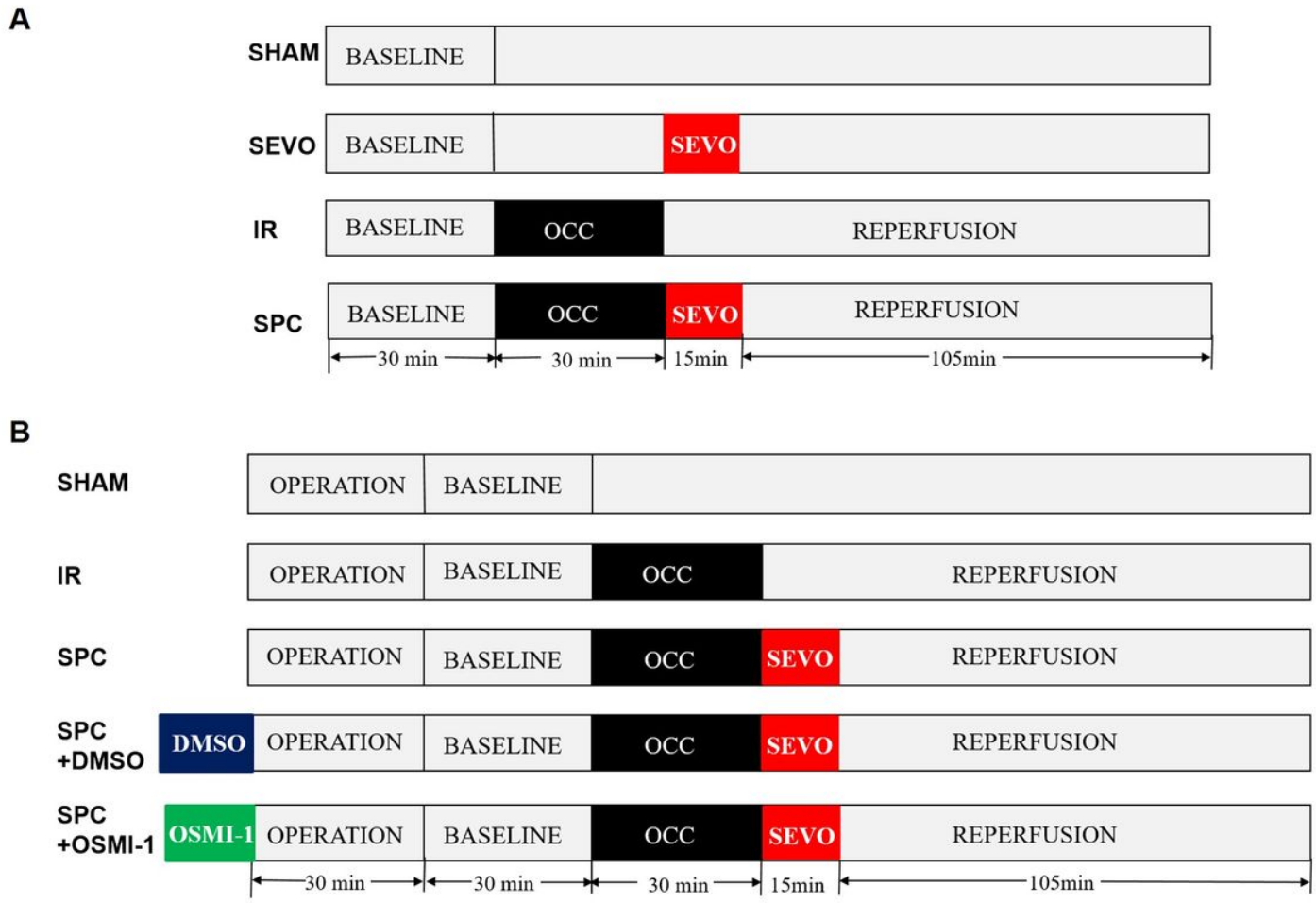


**Fig.1**

## Figure 1

Experimental procedures, general characteristics and the plasma level of H2S. a Schematic illustration of the experimental protocol in diabetic rats hearts. The red area represents ischemia time; the black area represents reperfusion time; the purple area represents saline administration 5days (i.p.); the yellow area represents 2.5% sevoflurane administration; the blue area represents 133mmol/kg H2S donor GYY4137 administration 5days (i.p.); the green area represents 5mg/kg EX527 administration 5days (i.p.). b-d Rats' food intake, water intake and blood glucose were recorded at the start (baseline) and the beginning of the ischemia (week 4). n = 10-12 /group. e The level of plasma H2S concentration was measured. n = 6-9 /group. *P0.05 vs Sham group; # P0.05 vs I/R group; Δ P0.05 vs SPC group; Values are expressed as the mean ± SD.

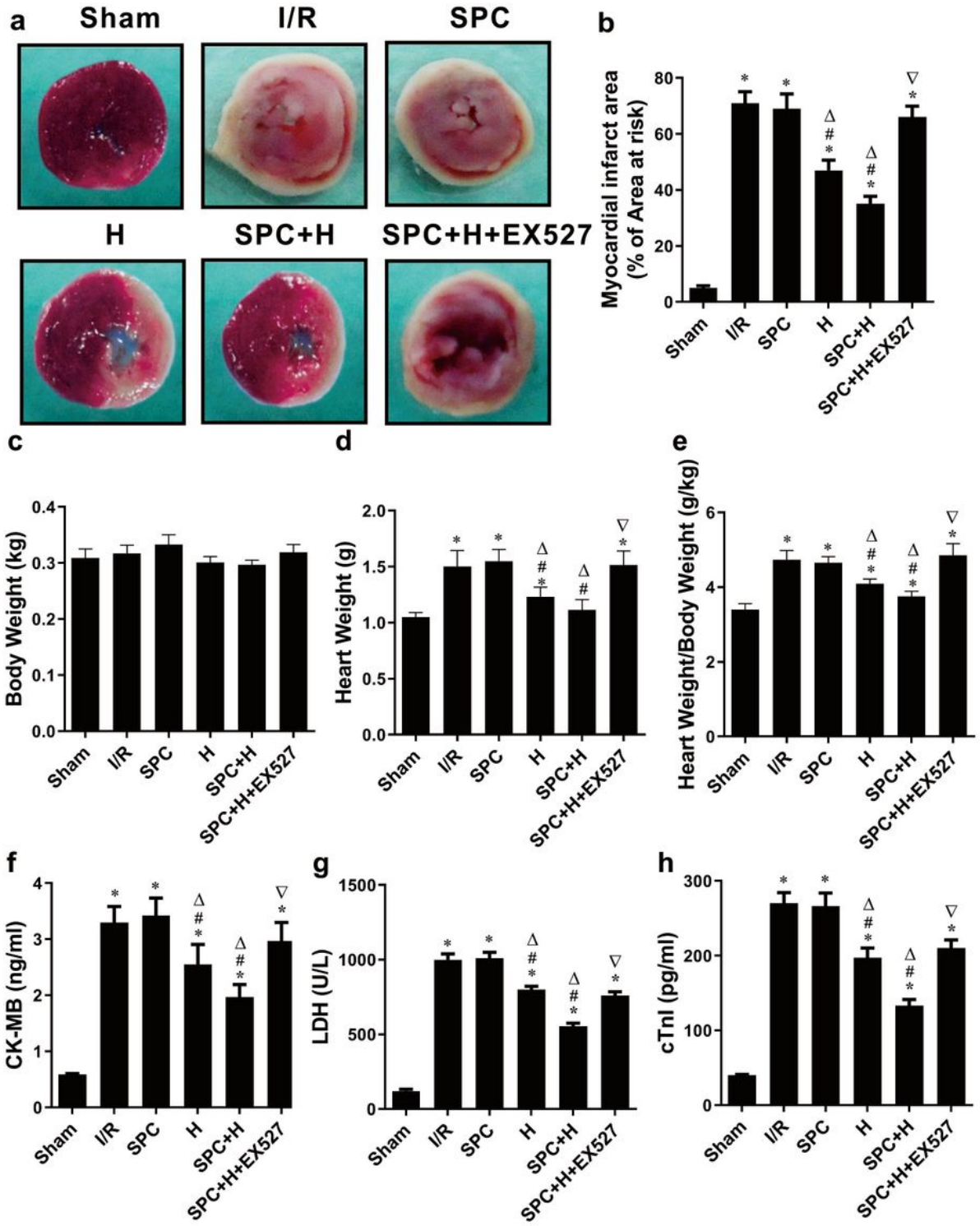


## Figure 2

GYY4137 enabled SPC to attenuate myocardial IRI-induced cardiac infarction size and cardiac dysfunction in diabetic rats but was abolished by inhibition of SIRT1. The effects of SPC and GYY4137 on myocardial infarction size and serum CK-MB, LDH and cTnI activities with or without the treatmnet of EX527 in IR-injured diabetic heart. a Representative images of TTC staining after reperfusion are shown. The red area represents normal myocardial tissue, and the pale area is the infarction and ischemia region.

b Myocardial infract area (% of Area at risk). n = 6 /group. c-e Diabetic rats' body weight, heart weight and heart weight/body weight were measured. n = 10-12 /group. f-h The levels of CK-MB, LDH and cTnI were detected. n = 6 /group. *P▯0.05 vs Sham group; # P▯0.05 vs I/R group; Δ P▯0.05 vs SPC group; ∇ P▯0.05 vs SPC+H group; Values are expressed as the mean ± SD.

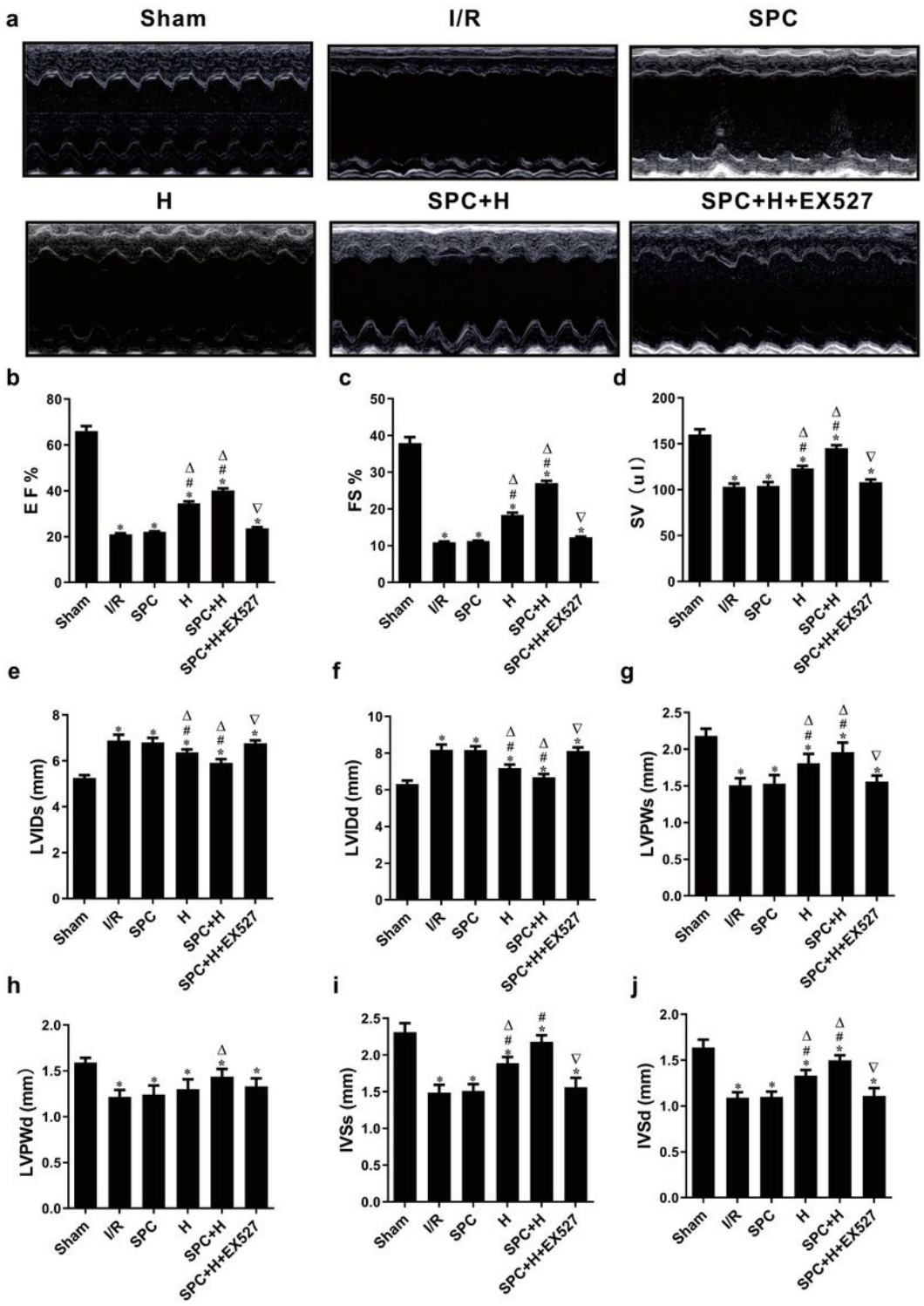


**Figure 3**

GYY4137 facilitated SPC to attenuate myocardial IRI-induced cardiac dysfunction in diabetic rats. The effects of SPC and GYY4137 on cardiac function with or without the treatmnet of EX527 in IR-injured diabetic heart. a Representative M-mode images of echocardiography are shown. b-j EF%, FS%, SV, LVIDs, LVIDd, LVPWs, LVPWd, IVSs and IVSd were measured and calculated n = 10-12/group. *P⍰0.05 vs Sham group; # P⍰0.05 vs I/R group; Δ P⍰0.05 vs SPC group; ∇ P⍰0.05 vs SPC+H group; Values are expressed as the mean ± SD.

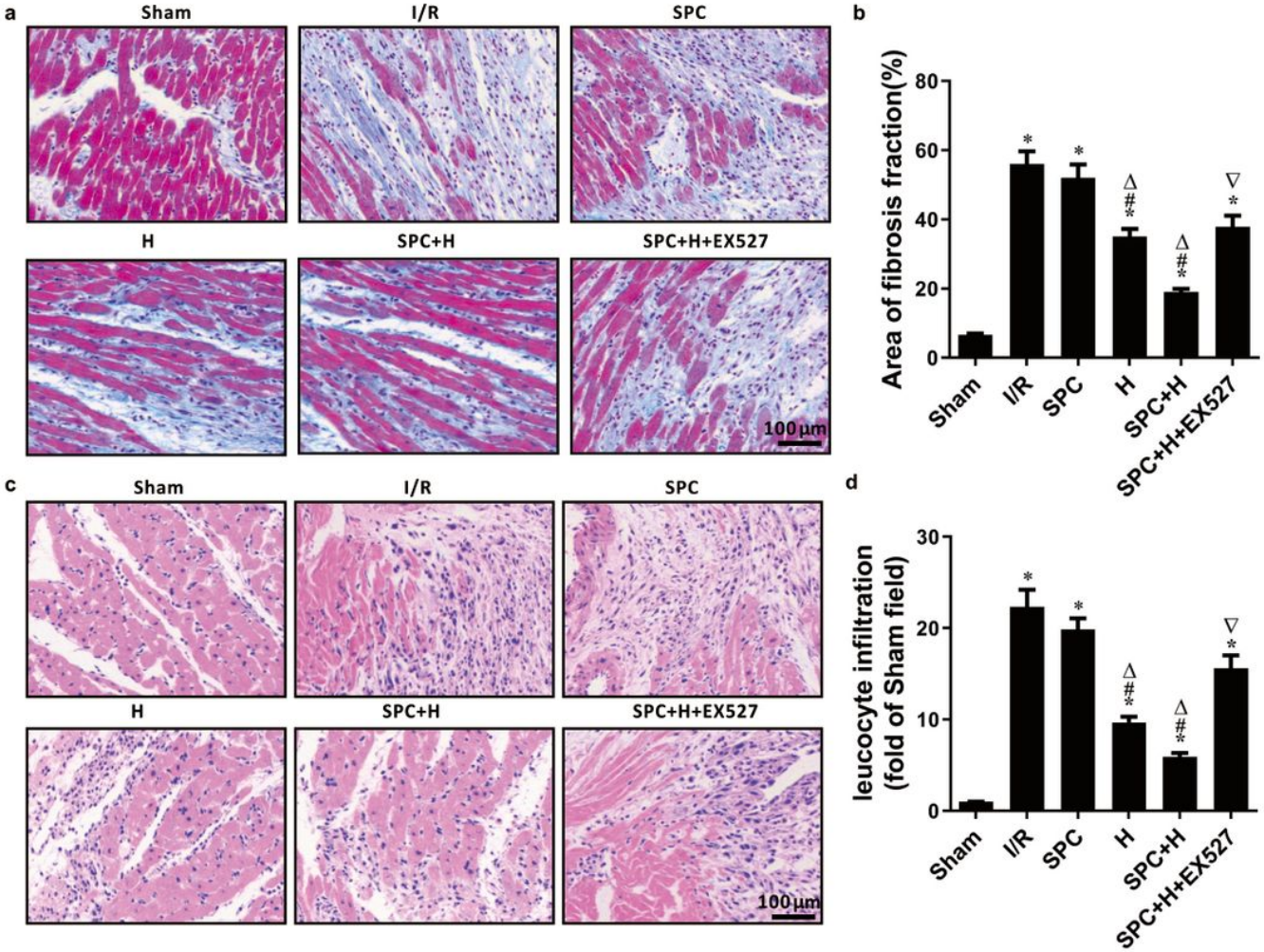


## Figure 4

GYY4137 restored SPC-induced cardioprotective effects in diabetic condition via suppress IRI myocardial damage and fibrosis. The effects of SPC and GYY4137 on cardiac tissue damage and fibrosis with or without the treatmnet of EX527 in IR-injured diabetic heart. a Representative images of myocardial fibrosis stained with the Masson method, Magnification 200x, scale bar = 100μm. b Quantitative analysis of area of fibrosis fraction. n = 4 /group. c Representative pictures of HE stained cardiac sections, Magnification 200x, scale bar = 100μm. d Quantitative analysis of leucocyte infiltration. n = 4 /group. *P⍰0.05 vs Sham group; # P⍰0.05 vs I/R group; Δ P⍰0.05 vs SPC group; ∇ P⍰0.05 vs SPC+H group; Values are expressed as the mean ± SD.

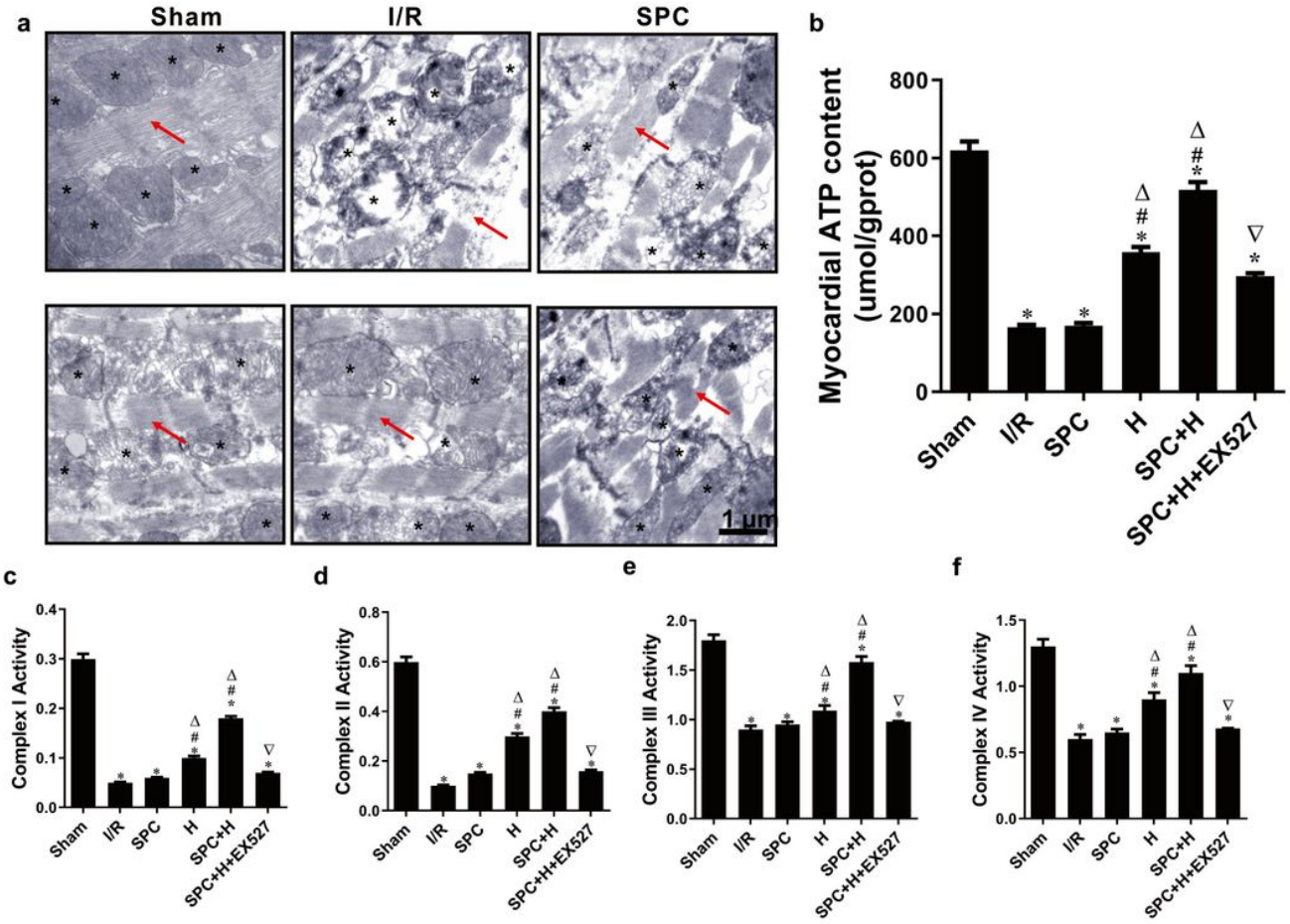


## Figure 5

Impaired mitochondrial structure and function in diabetic hearts were effectively recovered by the co-administration of SPC and GYY4137. The effects of SPC and GYY4137 on mitochondrial structure and function with or without the treatmnet of EX527 in IR-injured diabetic heart. a Representative transmission electron micrographs at a magnification of 20000, scale bar = 100μm. Note that myofilaments were absent (*) and mitochondria was damaged (→). n=3/group. b Quantitative analysis of myocardial ATP content. n = 6 /group. c-f Quantitative analysis of myocardial mitochondrial respiratory chain complex I, II, III and IV. n = 6 /group. *P 0.05 vs Sham group; # P 0.05 vs I/R group; Δ P 0.05 vs SPC group; ∇ P 0.05 vs SPC+H group; Values are expressed as the mean ± SD.

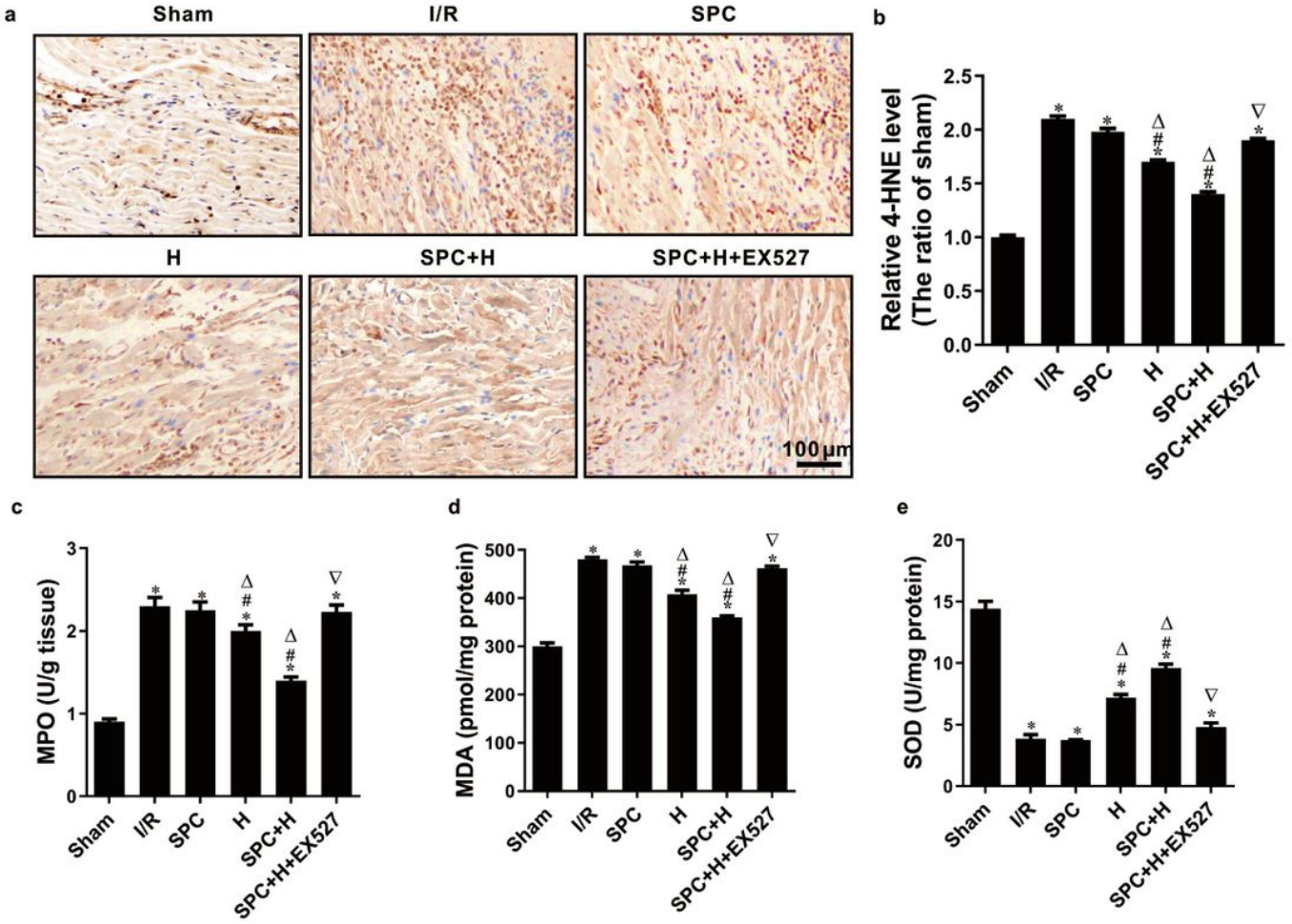


## Figure 6

SIRT1 regulated ROS generation and the expression of MPO, MDA and SOD participates in the effect of H2S to restore the SPC cardioprotection in diabetic rats. The effects of SPC and GYY4137 on oxidative stress and the level of MPO, MDA and SOD with or without the treatmnet of EX527 in IR-injured diabetic heart. a Representative immunohistochemistry staining at a magnification of 200, scale bar = 100μm. b Quantitative analysis of relative 4-HNE level. n=6/group. n= 4 /group. c-e Quantitative analysis of myocardial MPO, MDA and SOD levels. n= 6 /group. *P 0.05 vs Sham group; # P 0.05 vs I/R group; Δ P 0.05 vs SPC group; ∇ P 0.05 vs SPC+H group; Values are expressed as the mean ± SD.

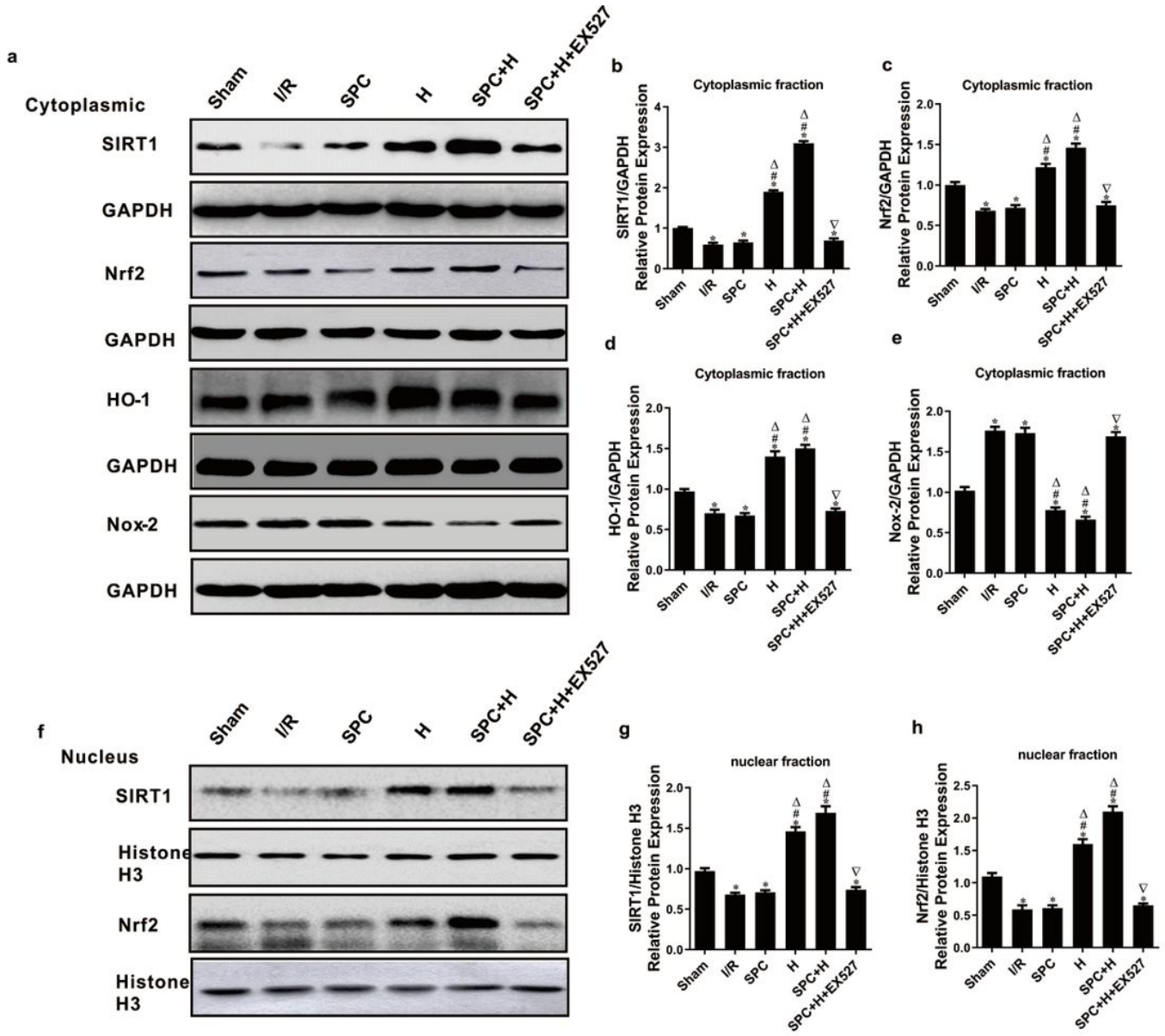


## Figure 7

GYY4137 restored the protective properties of SPC against diabetic myocardial IRI by enhancing SIRT1-modulated Nrf2/HO-1/Nox-2 signaling. The effects of SPC and GYY4137 on SIRT1 intracellular distribution and Nrf-2/HO-1 signaling with or without the treatmnet of EX527 in IR-injured diabetic heart. a Representative immunoblotting for cytoplasmic SIRT1, Nrf2, HO-1 and Nox-2 was performed. b-e The expressions of cytoplasmic SIRT1, Nrf2, HO-1 and Nox-2 were analyzed. n= 4 /group. f Representative immunoblotting for nucleus SIRT1 and Nrf2 was performed. g-h The expressions of nucleus SIRT1 and Nrf2 were analyzed. n= 4 /group. *P0.05 vs Sham group; # P0.05 vs I/R group; Δ P0.05 vs SPC group; ∇ P0.05 vs SPC+H group; Values are expressed as the mean ± SD.

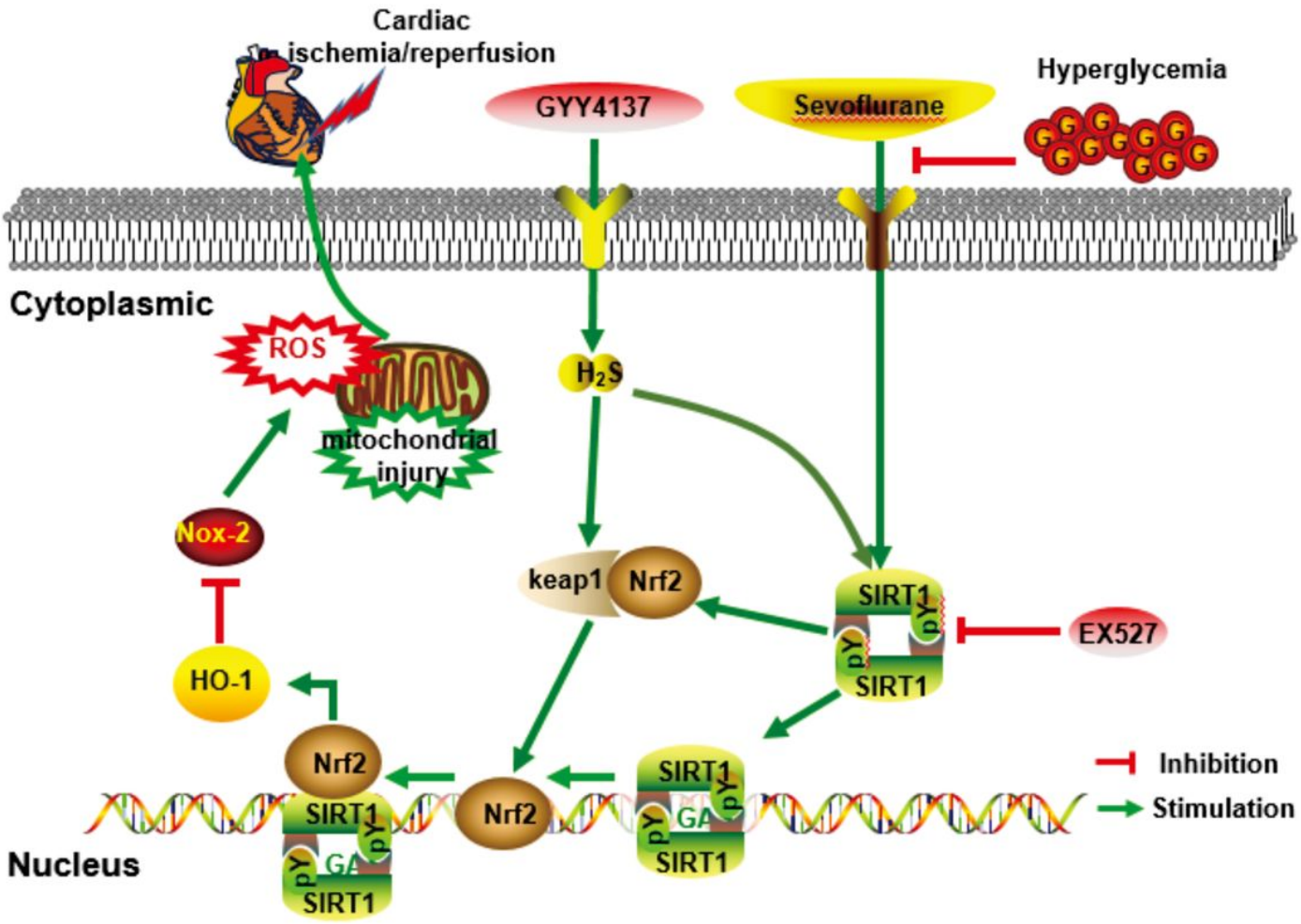


## Figure 8

The schematic diagram of exogenous H2S restoring SPC-induced cardioprotection in diabetic heart IRI via SIRT1-regulated Nrf2/HO-1/Nox-2 signaling pathway activation. Solid green arrows depict promotion, positive regulation or activation. Transverse red“T” shape indicates inhibition, negative regulation or blockade.